Visco-acoustic Reverse-time Migration with Finite-differences

Siwei Li, Guojian Shan and Yue Wang, Chevron Energy Technology Company

SUMMARY

Wave propagation in viscous medium is subject to amplitude dissipation and velocity dispersion. In this work, we adopt the theory of constant-Q model to describe visco-acoustic mechanism and propose a reverse-time migration that performs inverse-Q filtering along wave-paths, in order to compensate for dimmed and defocused image areas affected by Q anomalies. Considering practical cost-effectiveness, we have intentionally built our method on top of existing time-domain finite-difference wave propagators. For forward modeling, we fit a set of optimized Generalized Maxwell Body to constant-Q model in the seismic bandwidth and implement it by auxiliary first-order partial differential equations. By doing so, we avoid fractional time derivative and pseudo-differential operators that are computationally intensive. During migration, wavefields with and without Q are combined to inverse Q-dissipation while preserving Q-dispersion. For this procedure to be efficient and stable, we apply time-frequency analysis to account for non-stationarity and use smoothing to regularize spatial discontinuities. The independently processed source and receiver wavefields are suitable for usual cross-correlation or Laplacian imaging condition, where finally viscous effects along wave-path are accounted for.

INTRODUCTION

Recent developments of seismic imaging techniques have a trend towards more sophisticated physics in order to reconstruct wave propagation in complex geological models with high fidelity. It is well-known that elastic wave equation is insufficient in characterizing viscous medium, which naturally attenuates and distorts wavelet (Aki and Richards, 2002). Such phenomenon is very common in global seismological observations. In exploration geophysics, a typical example of viscous in-elasticity is shallow gas pockets. Their presence would usually degrade image qualities, resulting in weaker amplitude and narrower bandwidth.

When it comes to the theory of elasticity, there seems little debate on following Hooke's Law and Newton's Second Law. However for viscous in-elasticity, we have found several mechanisms proposed by various authors. Among the candidates, four are popular among exploration geophysicists: Standard Linear Solid (Robertsson et al., 1994; Larsen and Grieger, 1998), Generalized Maxwell Body (Flugge, 1975), constant-Q model (Kjartansson, 1979) and nearly-constant-Q model (Futterman, 1962). These mechanisms are parameterized such that for a given seismic bandwidth they all could potentially fit observations well. In fact, numerous publications have confirmed their applicability by comparing with laboratory experiments or seismological records (Christensen, 2010). Evaluating these mechanisms is critical for us to distinguish between Q-dissipation and Q-dispersion and to quantify the amount of reasonable corrections from Q reverse-time migration (RTM). Our current work is based on constant-Q model (CQ), but it turns out that mathematically these mechanisms are closely related. Unfortunately, a rigorous realization of CQ introduces fractional time derivative (Caputo and Mainardi, 1971). For Q RTM, we prefer time-domain finite-difference (TDFD) wave propagators, but a discretized fractional time derivative is sizable and hardly computationally favorable (Carcione, 1990). Chen and Holm (2004) recasted fractional time derivative as fractional Laplacian and solved it by Fourier pseudo-spectral method. Fractional Laplacian also appears in the work of Zhang et al. (2010) and Zhu and Harris (2014), who approximated CQ by slight linearization to decouple Q-dispersion and Q-dissipation. Yet these approaches are still quite costly, particularly because an inhomogeneous Q model makes the fractional Laplacian a mixed space-wavenumber domain pseudo-differential operator (Sun et al., 2014).

A desired Q RTM should remove viscous effects and result in an image as if the data were acquired in a non-viscous media. For Kirchhoff-type migrations, an inverse-Q filter is applied to input traces before imaging to correct for amplitude and phase (Bale and Jakubowicz, 1986; Hargreaves and Calvert, 1991; Wang, 2002). Under the assumption of weak Q-dispersion, the filter can be designed by accumulating Q along ray-path that connects source, subsurface image location and receiver in the background elastic model. The difficulties are instability when boosting up signals and non-stationarity in both space and time. The first problem is conveniently avoided by setting a gain limitation, while temporal non-stationarity is handled by filter banks or interpolation. Since a Q model is usually much smoother than velocity, the filter is seldom constrained by spatial continuity. The most straightforward idea of Q RTM is to incorporate inverse-Q filter into wave equation (Dai and West, 1994). This clearly requires not only forward CQ modeling but also a modified wave equation that keeps Q-dispersion while reversing Q-dissipation. For example, Zhu (2015) used the decoupled equation of Zhu and Harris (2014) with opposite sign of Q-dissipation for imaging. Zhang et al. (2010), Suh et al. (2012) and Bai et al. (2013) also derived equations with pseudo-differential operator for the same purpose, although they varied in underlying visco-elastic mechanisms. Besides the challenge in TDFD implementation, an additional and non-trivial issue arises in stabilizing the propagator so that high frequency contents do not grow out of control.

Alternatively, one may seek a work-around for Q RTM by applying inverse-Q filtering along wave-paths (Fletcher et al., 2012). Similarly to ray-path tracing for Q Kirchhoff-type migration, we can ignore wave-path changes due to Q-dispersion and attempt to estimate the accumulated Q by comparing wavefields simulated with and without Q. On one hand, the wavefield with Q is attainable from forward CQ modeling and free of instability. On the other hand, extracting information from

wavefields is perceivably problematic, especially for the receiver side. For example, Nichols (1996) calculated most energetic arrivals from solutions of Helmholtz equation, and performed a parametric fit to condition the traveltime picks before passing them to Kirchhoff migration. Nonetheless, the tedious and error-prone procedure for finding wave-paths is not mandatory for Q RTM. As long as we could effectively separate Q-dispersion and Q-dissipation, a direct compensation only for dissipation is sufficient. Xie et al. (2015) first applied Fourier transform in time to traces at each subsurface location, then reshaped spectrum of viscous wavefield according to its loss with respect to non-viscous wavefield. Following these works, our current interest is an intermediate solution that stays as close to the cost of TDFD propagator as possible but delivers better, albeit not ultimate, Q compensation for imaging purposes.

The paper will start with a visco-acoustic TDFD forward modeling. Next, we analyze how Q compensation might be done by spectral reshaping and discuss imaging condition for Q RTM. The proposed method is explained by synthetic datasets. Finally, we conclude the paper after some discussions.

VISCO-ACOUSTIC MODELING

Our choice of TDFD modeling is based on Generalized Maxwell Body (GMB), specifically a GMB that approximates CQ in the frequency range of interest. A L-component GMB has a relaxation function spectrum that consists of L single peaks of weight y_l at discrete relaxation frequencies ω_l, i.e.

$$M_{\text{GMB}}(\omega) = M_U \left(1 - \frac{\sum_{l=1}^{L} y_l \dfrac{\omega_l}{i\omega + \omega_l}}{1 + \sum_{l=1}^{L} y_l} \right) , \tag{1}$$

where M_U is the unrelaxed modulus. Moczo and Kristek (2005) proved analytically that GMB and so-called Generalized Zener Model (GZM) were equivalent, where Standard Linear Solid (SLS) is a special case of GZM with $L = 1$ and

$$\begin{aligned} M_U &= (1 + y_1)\, k_0 \,, \\ y_1 &= \tau_\varepsilon \tau_\sigma^{-1} - 1 \,, \\ \omega_1 &= \tau_\sigma^{-1} \,. \end{aligned} \tag{2}$$

By definition

$$Q^{-1}(\omega) = \frac{\Im(M)}{\Re(M)} \tag{3}$$

and thus (Emmerich and Korn, 1987)

$$\sum_{l=1}^{L} \frac{\omega_k \left[\omega_l - \omega_k Q_{\text{GMB}}^{-1}(\omega_k) \right]}{\omega_l^2 + \omega_k^2} y_l = Q_{\text{GMB}}^{-1}(\omega_k) \,, \tag{4}$$

where $k = 1, 2, \ldots, K$. To fit CQ, we let $Q_{\text{GMB}}(\omega_k) \equiv Q$. For known $K \geq L$ and ω_l, equation 4 is an over-determined linear system for y_l and can be solved by least-squares. For large Q, ω_l can be conveniently chosen in logarithmic scale thanks to the symmetry of Debye functions. For small Q such as $Q < 20$, we find an additional non-linear optimization after solving 4 is helpful for keeping L as few as possible while achieving satisfying modeling accuracy.

$$C(\mathbf{y}_l, \omega_l) = \frac{1}{2} \sum_{k=1}^{K} \| Q_{\text{GMB}}^{-1}(\omega_k) - Q^{-1} \|^2 \,. \tag{5}$$

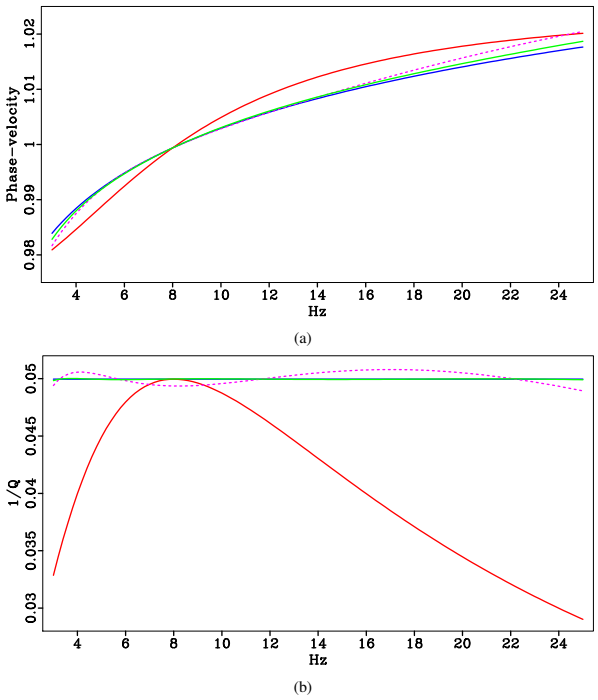

Figure 1: Comparisons of CQ approximations in (top) dispersion and (bottom) dissipation. We choose $c_r = 1$, $Q = 20$ and $f_r = 8$ Hz. The range of frequencies is relevant to a typical 25 Hz RTM. The small f_r is not necessarily practical but is helpful in terms of high-lighting features of approximations. Solid blue: CQ. Solid red: SLS. Dashed magenta: GMB. Solid green: GMB with optimization.

In the CQ model proposed by Kjartansson (1979)

$$M_{\text{CQ}}(\omega) = c_r^2 \cos^2\left(\frac{\pi\gamma}{2}\right) \left(\frac{i\omega}{\omega_r}\right)^{2\gamma} , \tag{6}$$

where

$$\gamma = \frac{1}{\pi} \arctan\left(\frac{1}{Q}\right) , \tag{7}$$

there are two additional parameters c_r and ω_r. From a physicist's point of view, c_r, ω_r and Q are properties of rocks, just

as density and elastic modulus. If they are to be determined in laboratory, their values can be tuned to fit the relaxation function measured from a rock sample. Previous works on inverse-Q filters usually specify c_r as elastic velocity and set ω_r to be the high-end of seismic frequency band. Currently, Q is estimated from tomography and is most of time solely amplitude based. Meanwhile, ω_r has significant impact on Q dispersion: if $Q = 20$ and $c_r = 1$, the phase velocity difference between $\omega_r = 20$ and 250 can be nearly 5%. Because gathers are flattened already during velocity model building and we do not expect Q-dispersion to be responsible for any residual curvature, it is reasonable to assign c_r migration velocity and restrict ω_r around dominant frequency of data. Consequently, we adjust M_U to match CQ phase velocity at ω_r. Figure 1 compares different approximations of CQ.

Expression 1 can now be inserted into acoustic wave equation, which leads to rather simple implementation with the help of so-called memory variable (Day and Minster, 1984; Carcione, 1990). Interestingly, not only the governing first-order partial differential equation but also its TDFD implementation on top of an existing TDFD wave propagator are similar to convolutional perfectly matched layer (PML) (Roden and Gedney, 2000). Indeed, one of the outstanding merit of PML is its uniform damping with respect to frequencies. CQ, on the other hand, is biased towards higher frequencies. In Figure 2 we benchmark our Q modeling against that by fractional Laplacian through pseudo-spectral (Sun et al., 2014). Because an additional $3L$ memories of wavefield size are required, a smaller L is always preferable for computational efficiency.

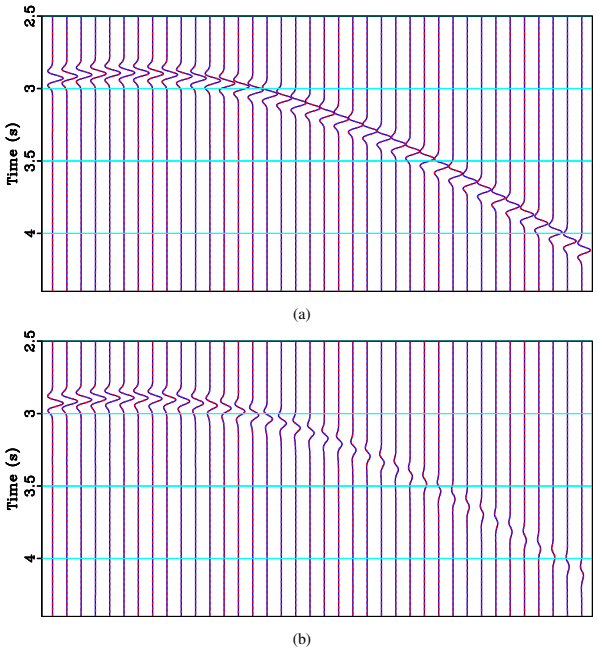

Figure 2: CQ synthesizing with optimized GMB (solid blue) and fractional Laplacian (dashed magenta). Compare (a) acoustic and (b) visco-acoustic cases with a minimum $Q = 10$ Gaussian anomaly model. Velocities are constant in both cases.

IMAGING CONDITION WITH Q COMPENSATION

From inverse-Q Kirchhoff to Q RTM, ideally we want finite bandwidth wave-path taking the place of ray-path. Following inverse-Q filtering (Wang, 2002) and using WKBJ ansatz for wavefield (Bleistein et al., 2001), the acoustic wavefield P_0 and visco-acoustic wavefield P_{CQ} are

$$P_0 = A \cdot \exp(-i\omega T)\,, \tag{8}$$

$$P_{\mathrm{CQ}} = A \cdot \exp\left(-i\omega T + i\omega \frac{1}{\pi} T^* \ln\left|\frac{\omega}{\omega_r}\right| - \frac{1}{2}\omega T^*\right) \tag{9}$$

respectively. Here T^* is the linearized traveltime perturbation due to Q. Meanwhile, Q-compensated wavefield that is desired by imaging purposes reads

$$P_c = A \cdot \exp\left(-i\omega T + i\omega \frac{1}{\pi} T^* \ln\left|\frac{\omega}{\omega_r}\right| + \frac{1}{2}\omega T^*\right)\,. \tag{10}$$

It turns out that a GMB matched to equation 10 is numerically unstable, even in a simplest homogeneous Q model. However, P_c is related to P_0 and P_{CQ} through (Xie et al., 2015)

$$P_c = \left|\frac{P_0}{P_{\mathrm{CQ}}}\right|^2 P_{\mathrm{CQ}}\,. \tag{11}$$

Equation 11 indicates comparing acoustic and visco-acoustic wavefields in the Fourier domain to separate out and compensate for Q-dissipation. Note that this spectral reshaping of P_{CQ} is done per each ω, as Q-dispersion and Q-dissipation are frequency dependent. The major trouble of equation 11 is failure to account for multiple arrivals and non-uniform distribution of Q effects. In Figure 3 we synthesize a single trace containing two Ricker arrivals using equations 8 to 10. p_{CQ} (not shown) has symmetric shape as p_c because Q-dispersion is automatically corrected by wave propagation. Applying equation 11 results in a leakage of spectral energy causes an artifact at around $t = 1.4$ s. These artifacts in fact appear throughout the whole trace and will be falsely cross-correlated during imaging condition. We mitigate such artifacts by applying 11 in an efficient time-frequency analysis. An underlying assumption we must bear in this process is that Q anomaly model shall be smooth, which is usually valid considering practical tomographic Q estimation. Another possible refinement of 11 is to replace p_0 by another p^*_{CQ} with slightly perturbed Q model, for example a 1% increase. Depending on complexity of Q model, this may help improve accuracy because we are implicitly comparing two potentially distinctive wave-paths.

Another issue arises during imaging condition, such as Laplacian and inverse scattering. These imaging conditions require p_c to be differentiable, but this seemingly trivial property is not generally guaranteed. The root of problem is a location-wise operation by 11. Figure 4 (a) plots the scalar multiplied to

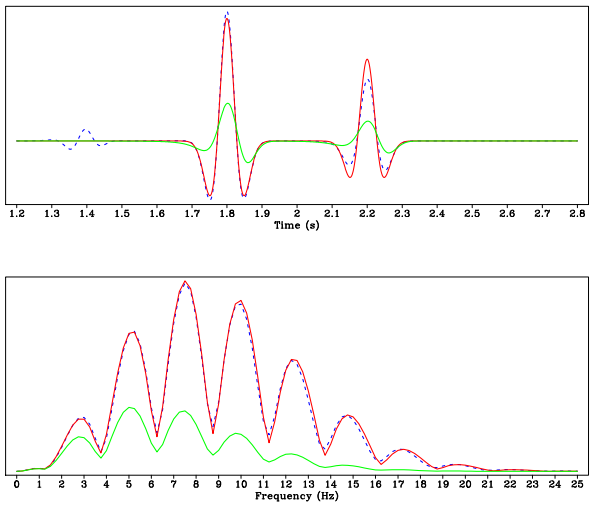

Figure 3: p_c (dashed blue) computed by equation 11. Solid red is analytical solution (i.e. ground truth) and solid green in p_0.

p_{CQ} for Q-dissipation compensation in a simple 2D Gaussian anomaly model. Note spectrums of p_0 and p_{CQ} are oscillatory due to nature of Green's function. Discontinuity in space is visible, especially where abrupt branch change happens. Similar problem is expected in deconvolutional imaging condition. A sophisticated 2D or 3D regularization shall be effective here, but we realize it is not attractive given our primary concern on a minimum cost. For this reason, we chain simpler but much more efficient 1D weighted smoothing along each dimension to suppress spatial discontinuities in p_c.

Lastly, we demonstrate the proposed Q RTM with Marmousi 2 model (Bourgeois et al., 1991). We use a $[3,5,50,55]$ Hz Ormsby wavelet and $f_r = 50$ Hz for modeling and migration. Q model has a Gaussian anomaly at $(z,x) = (1.5,9)$ km. Figure 5 compares RTM and Q RTM images.

CONCLUSIONS

We have proposed a Q RTM that may potentially be built upon existing TDFD RTM. The general idea is to first perform inhomogeneous Q modeling with a cost comparable to non-viscous modeling, then apply a post-processing on wavefields to correct for Q dissipation while keeping Q dispersion. There are two major challenges, namely the non-stationarity of post-processing in both time and space. In time, we must address multiple arrivals and variable accumulated Q effects. And in space, discontinuity due to noisy division and branch jumping may become artifacts in final image after imaging condition.

ACKNOWLEDGMENTS

The authors wish to thank Chevron Energy Technology Company for permission to publish this work. We would like to thank Lin Zhang, Gilles Hennenfent and Yonghe Sun for inspiring discussions.

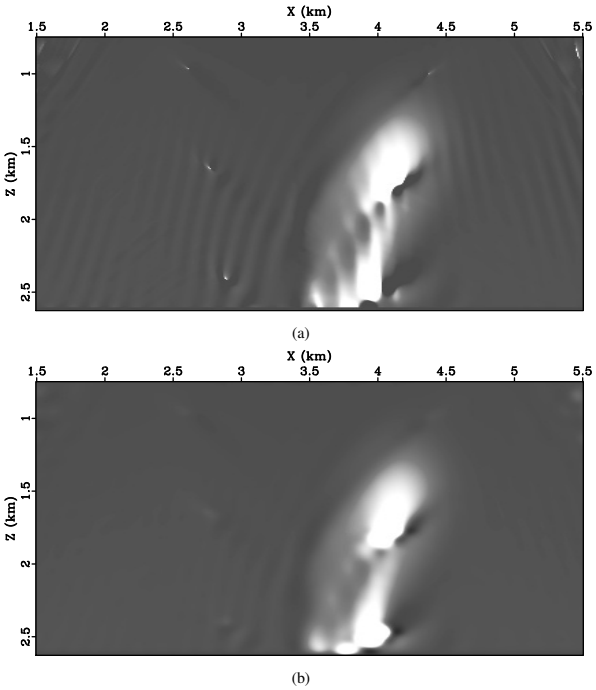

Figure 4: Scalar applied to p_{CQ} near 1 s and 10 Hz for inverse Q-dissipation. (a) Without and (b) with smoothing.

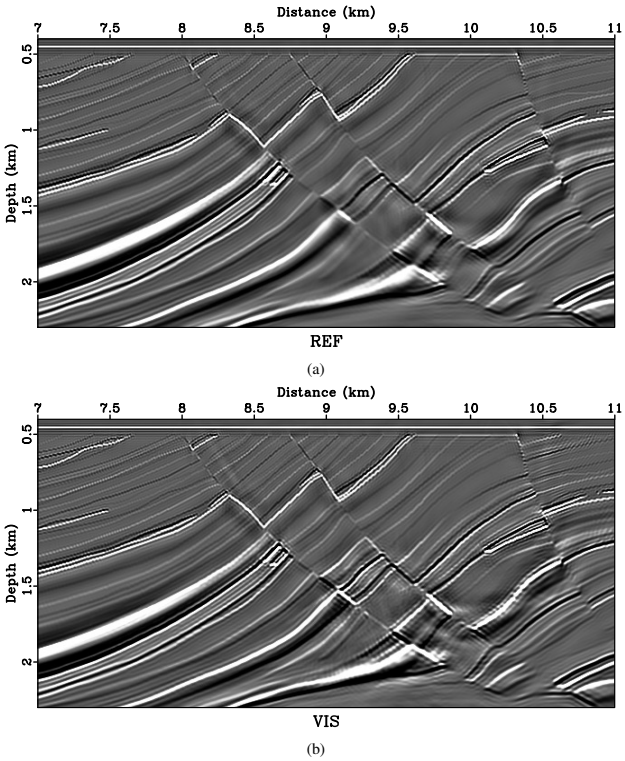

Figure 5: Images from (a) RTM and (b) Q RTM, both with Laplacian imaging condition.

EDITED REFERENCES

Note: This reference list is a copyedited version of the reference list submitted by the author. Reference lists for the 2017 SEG Technical Program Expanded Abstracts have been copyedited so that references provided with the online metadata for each paper will achieve a high degree of linking to cited sources that appear on the Web.

REFERENCES

Aki, K., and P. G. Richards, 2002, Quantitative seismology: University Science Books.

Bai, J., G. Chen, D. Yingst, and J. Leveille, 2013, Attenuation compensation in viscoacoustic reverse-time migration: 83rd Annual International Meetings, SEG, Expanded Abstracts, 1252.

Bale, R., and H. Jakubowicz, 1986, Inverse Q filtering of seismic data: 56th Annual International Meetings, SEG Expanded Abstracts, 512–514.

Bleistein, N., J. K. Cohen, and W. J. Stockwell, 2001, Mathematics of multidimensional seismic imaging, migration, and inversion: Springer.

Bourgeois, A., M. Bourget, P. Lailly, M. Poulet, P. Ricarte, and R. Versteeg, 1991, The Marmousi experience: Proceedings of the 1990 EAEG workshop: EAGE, Marmousi, model and data, 5–16.

Caputo, M., and F. Mainardi, 1971, A new dissipation model based on memory mechanism: Pure and Applied Geophysics, **91**, 134–147, https://doi.org/10.1007/BF00879562.

Carcione, J. M., 1990, Wave propagation in anisotropic linear viscoelastic media: Theory and simulated wavefields: Geophysical Journal International, **101**, 739–750, https://doi.org/10.1111/j.1365-246X.1990.tb05580.x.

Chen,W., and S. Holm, 2004, Fractional Laplacian time-space models for linear and nonlinear lossy media exhibiting arbitrary frequency power-law dependency: Journal of the Acoustical Society of America, **115**, 1424–1430, https://doi.org/10.1121/1.1646399.

Christensen, R. M., 2010, Theory of Viscoelasticity: Dover Publications Inc.

Dai, N., and G. F. West, 1994, Inverse Q migration: 64th Annual International Meetings, SEG Expanded Abstracts, 1418–1412.

Day, S. M., and J. B. Minster, 1984, Numerical simulation of attenuated wavefields using a Pade approximation method: Geophysical Journal of the Royal Astronomy Society, **78**, 105–118, https://doi.org/10.1111/j.1365-246X.1984.tb06474.x.

Emmerich, H., and M. Korn, 1987, Incorporation of attenuation into time-domain computations of seismic wave fields: Geophysics, **52**, 1252–1264, https://doi.org/10.1190/1.1442386.

Fletcher, R. P., D. Nichols, and M. Cavalca, 2012, Wavepath consistent effective Q estimation for Q-compensated reverse-time migration: 74th Annual International Conference and Exhibition, EAGE, Extended Abstracts incorporating SPE EUROPEC, https://doi.org/10.3997/2214-4609.20148360.

Flugge, W., 1975, Viscoelasticity: Springer.

Futterman, W. I., 1962, Dispersive body waves: Journal of Geophysical Research, **67**, 5279–5291, https://doi.org/10.1029/JZ067i013p05279.

Hargreaves, N. D., and A. J. Calvert, 1991, Inverse Q filtering by Fourier transform: Geophysics, **56**, 519–527, https://doi.org/10.1190/1.1443067.

Kjartansson, E., 1979, Constant Q-wave propagation and attenuation: Journal of Geophysical Research, **84**, 4737–4748, https://doi.org/10.1029/JB084iB09p04737.

Larsen, S., and J. Grieger, 1998, Elastic modeling initiative: Part 3 — 3-D computational modeling: 68th Annual International Meetings, SEG Expanded Abstracts, 1803–1806, https://doi.org/10.1190/1.1820281.

Moczo, P., and J. Kristek, 2005, On the rheological models used for time-domain methods of seismic wave propagation: Geophysical Research Letters, **32**, L01306, https://doi.org/10.1029/2004GL021598.

Nichols, D. E., 1996, Maximum energy traveltimes calculated in the seismic frequency band: Geophysics, **61**, 253–263, https://doi.org/10.1190/1.1443946.
Robertsson, J. O. A., J. O. Blanch, and W. W. Symes, 1994, Viscoelastic finite-difference modeling: Geophysics, **59**, 1444–1456, https://doi.org/10.1190/1.1443701.
Roden, J. A., and S. D. Gedney, 2000, Convolutional PML (CPML): An efficient FDTD implementation of the CFSPML for arbitrary media: Microwave and Optical Technology Letters, **27**, 334–339, https://doi.org/10.1002/1098-2760(20001205)27:5<334::AID-MOP14>3.0.CO;2-A.
Suh, S., K. Yoon, J. Cai, and B. Wang, 2012, Compensating visco-acoustic effects in anisotropic reverse-time migration: 82nd Annual International Meetings, SEG Expanded Abstracts, 1–5, https://doi.org/10.1190/segam2012-1297.1.
Sun, J., S. Fomel, and T. Zhu, 2014, Viscoacoustic modeling and imaging using low-rank approximation: 84th Annual International Meetings, SEG Expanded Abstracts, 3997–4002, https://doi.org/10.1190/segam2014-1596.1.
Wang, Y., 2002, A stable and efficient approach of inverse Q filtering: Geophysics, **67**, 657–663, https://doi.org/10.1190/1.1468627.
Xie, Y., J. Sun, Y. Zhang, and J. Zhou, 2015, Compensating visco-acoustic effects in TTI reverse time migration: 85th Annual International Meetings, SEG Expanded Abstracts, 3996–4001, https://doi.org/10.1190/segam2015-5855445.1.
Zhang, Y., P. Zhang, and H. Zhang, 2010, Compensating for visco-elastic effects with reverse time migration: 80th Annual International Meetings, SEG Expanded Abstracts, https://doi.org/10.1190/1.3513503.
Zhu, T., 2015, Viscoelastic time-reversal imaging: Geophysics, **80**, no. 2, A45–A50, https://doi.org/10.1190/geo2014-0327.1.
Zhu, T., and J. M. Harris, 2014, Modeling acoustic wave propagation in heterogeneous attenuating media using decoupled fractional Laplacians: Geophysics, **79**, no. 3, T105–T116, https://doi.org/10.1190/geo2013-0245.1.